APPLIED ELECTROCHEMISTRY
AND METAL CORROSION PROTECTION

Experimental and Computational Studies of *N*-(4,6-Dimethylpyrimidin-2-yl)-4-[(quinazoline-4-yl)amino]-benzene-1-sulfonamide as an Effectual Corrosion Inhibitor for Mild Steel in Hydrochloric Acid

Pramila Rita D'Souza[a], Jyothi Kudva[a],*, A. Sunil Kumar[a], and A. Nityananda Shetty[b]

[a] *Department of Chemistry, St Joseph Engineering College, Mangaluru, 575028 India*
[b] *Department of Chemistry, National Institute of Technology Karnataka, Surathkal, Mangaluru, 575025 India*
*e-mail: jyothikudva@gmail.com

Abstract—The inhibition efficacy of *N*-(4,6-dimethylpyrimidin-2-yl)-4-[(quinazoline-4-yl)amino]benzene-1-sulfonamide (DMQS) as a new corrosion inhibitor on mild steel (MS) in 0.1 M HCl medium at varied temperature has been analysed and it has ensued 97.6% high efficiency at 4×10^{-5} M of DMQS. The electrochemical techniques employed were impedance spectroscopy and potentiodynamic polarization. Surface analysis of MS was carried out through scanning electron microscopy (SEM) and energy dispersion spectroscopy (EDS). Inhibitory effect of DMQS escalated with elevated concentration and declined with elevation in solution temperature. The adsorption of DMQS on MS has consent with the Langmuir adsorption isotherm. The computational study using density functional theory (DFT) with the B3LYP/3-21G basis set level for DMQS was investigated through the association between their molecular and electronic structure. The parameters involved in quantum chemical calculations were energy gap, E_{HOMO}, E_{LUMO}, absolute electronegativity, electrophilicity, softness, global hardness, energy gap, ionisation energy, electron affinity and dipole moment. DMQS shows E_{HOMO} value of –6.256 eV, fortifying MS from corrosive attack and implicating it to be an effectual inhibitor. The results of the implemented studies show the corrosion inhibition efficiency of the DMQS is in good accord.

Keywords: MS, inhibition, DFT, corrosion, electrochemical techniques, quantum chemical parameters

DOI: 10.1134/S1070427221080140

INTRODUCTION

Industrial applications make use of MS as a constructional material for being economical and having exceptional mechanical properties. Organic inhibitors have a pivotal role in controlling corrosion of materials [1]. The physicochemical properties of the corrosion inhibitor like electron density of the donor atom, aromaticity, presence of pi electron in the double or triple bonds, presence of electronegative functional groups and its molecular structure attribute towards its adsorption on a metallic surface [2]. The heteroatoms like nitrogen, sulfur, phosphorous, oxygen etc., by virtue of its lone pair of electrons and planarity have proven to be chief centres for adsorption. The effectual mechanism can be elucidated through computational studies [3]. In general, sulfonamides have low potential for adverse health effects which is based on its history for safe therapeutic use in human beings [4, 5]. Sulfonamides are regarded to have eminent corrosion inhibition properties based on the facts that they are molecules having sulfur, nitrogen and oxygen heteroatoms that have lone pair of electrons, electron rich aromatic rings, the presence of multiple bonds, they are environmentally affable and they can be facilely synthesised. It has been indicative in earlier studies that an amide group present in the molecular scaffold of the inhibitor leads to its adsorption on the MS surface resulting in formation

of protective complexes which decline the rate of corrosion [6]. The crucial molecular framework in the core structure of Quinazoline derivatives among heterocyclic compounds present pharmacological properties of a wide range. The Quinazoline sulfonamide derivatives were synthesized and the structures were successfully characterised [7–9]. Corrosion inhibition study on MS in HCl by DMQS, which is a Quinazoline sulfonamide has been investigated in this paper. The objective of this study is to gain consensus to the efficacy of the inhibitor used to control corrosion on mild steel and to be able to utilise it in ameliorating the durability of metals.

Table 1. Elemental composition of MS

Element	Weight, %
C	0.234
Ni	0.61
Mn	0.016
Al	0.0027
Co	0.0065
P	0.012
Cr	0.025
Si	0.036
Fe	Rest

EXPERIMENTAL

Test material. The test material used for corrosion measurements was mild steel with chemical composition given in Table 1. The test material was a cylindrical rod cut and covered by acrylic repair material so that 0.6359 cm^2 surface area was in contact with the solution. The test material was polished using various grades of emery papers (500, 800, 1000, 1200, 1500, and 2000), cleaned with doubly distilled water, then by acetone wash, subsequently dried and stored in a desiccator until used for the experiment.

Medium. Preparation of 0.1 M HCl working solution was prepared by mixing 37% HCl (analytical grade) and adequate amount of double distilled water (ddH$_2$O). A stock solution of corrosion inhibitor (1×10^{-4} M) was prepared by the addition of ddH$_2$O. To facilitate thorough dissolution of the inhibitor compound, a ratio of 1 : 100 of DMSO and ddH$_2$O was employed. A series of concentrations from the stock solution were prepared (1×10^{-5}, 2×10^{-5}, 3×10^{-5}, and 4×10^{-5} M). The inhibitor used in this study was synthesised and its molecular structure was determined [7]. Figure 1 depicts the molecular structure of DMQS.

Electrochemical techniques. A CH-Instrument Model 608D series electrochemical workstation was used to carry out electrochemical measurements. The cell arrangement comprised of conventional three electrodes namely, saturated calomel electrode (reference electrode), platinum electrode (counter electrode) and test material (working electrode). The test material was covered by acrylic repair material so that only 0.6359 cm^2 surface area was in contact with the solution. The test material was polished using various grades of emery papers (500, 800, 1000, 1200, 1500, and 2000),

cleaned with doubly distilled water, then by acetone wash, subsequently dried and stored in a desiccator until used for the experiment. The measurements were done once the test solution attained stable open circuit potential and at atmospheric conditions without any stirring.

Electrochemical impedance spectroscopy (EIS). The well-polished test material was dipped in 0.1 M HCl with the inhibitor, varying concentration and at temperatures ranging from 303 to 323K. Electrochemical impedance curves were measured using 10 mV amplitude (peak to peak) and an AC signal over a frequency range of 100 000–0.1 Hz after an immersion period of 30 min. ZSimpWin version 3.21 software from the equivalent circuit were used to deduce the resistance due to charge transfer, R and the capacitance of double layer, C_{dl}.

Potentiodynamic polarization (PDP). Potentiodynamic polarization curves were measured using the smoothly polished test material dipped in 0.1 M HCl with the inhibitor, varying concentration, at temperature ranging from 303 to 323 K, at the potential range –250 to +250 mV and a scan rate of 1 mV/s.

Surface analysis. MS coupons of a surface area 0.6359 cm^2 were treated with 0.1 M HCl with the addi-
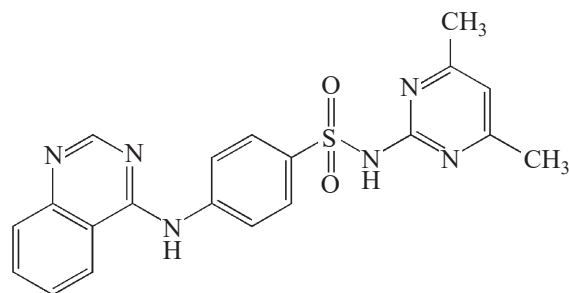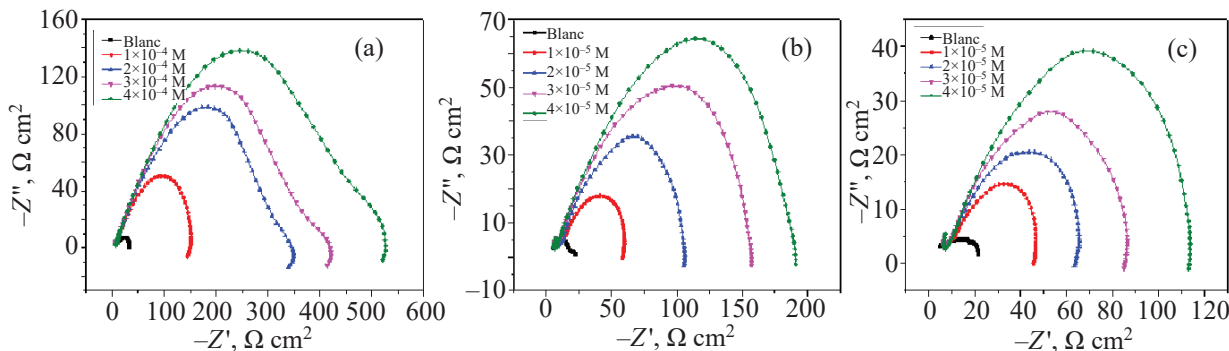

Fig. 1. Molecular structure of DMQS.

Fig. 2. (Color online) Nyquist plots of MS in 0.1 M HCl without the addition and with the addition of different concentrations of DMQS at (a) 303 (b) 313 and (c) 323 K.

tion and without the addition of DMQS at 303 K. JEOL JSM-6380L Field emission scanning electron microscope was employed in order to descry the morphology of the surface and analyse energy dispersive spectroscopy (EDS).

Computational methods. Effectuality of the inhibitor used was verified by carrying out density functional theory (DFT) and quantum chemical calculations. Gaussian 16W software package and GaussView 6.0 was utilised to draw the molecular sketches of DMQS. The DFT studies are done using correlation theory of Becke's three parameter and the Lee-Yang-Parr (B3L-YP) and by selecting a 3-21G basis set. It has been evident that DFT has profound implacability in the investigation of the characteristics relative to surface mechanisms of the metal-inhibitor and to the depiction of corrosion process being relative to the natural structure of the inhibitor [10, 11].

The quantum chemical parameters are calculated that include E_{HOMO} (energy relative to highest occupied molecular orbital), E_{LUMO} (energy relative to lowest unoccupied molecular orbital), energy gap (ΔE), ionisation potential (I), electronegativity (χ), softness (S), global hardness (η), dipole moment (μ), fraction of electrons

Fig. 3. Equivalent circuit employed to contour the EIS experimental results.

provided from the inhibitor to the metal surface (ΔN), electron affinity (A) and electrophilicity (ω).

RESULTS AND DISCUSSION

Electrochemical impedance spectroscopy (EIS). The efficacy of DMQS was evaluated from R_{ct} values and C_{dl} values of the impedance. The impedance spectra (Nyquist plots) of MS in 0.1 M HCl containing 0, 1×10^{-5} M, 2×10^{-5}, 3×10^{-5}, and 4×10^{-5} M of the DMQS at 303, 313, and 323 K is shown in Fig. 2. The imperfection in the semicircles of Nyquist Plot could be associated to the unevenness and non-uniformity in surfaces, adsorption of the DMQS and permeable layer formation [12, 13]. The display of Nyquist plot as bow-shaped indicates that during dissolution the occurrence of charge transfer [14]. The dimension of the semicircles escalates with a rise in DMQS concentration. The electrochemical impedance inhibition efficiency (IE, %) is calculated using Eq. 1, where R_{ct} and R^0_{ct} are the charge transfer resistance with the addition and without the addition of DMQS. Accordingly, the impact of temperature on corrosion suppression of MS with the addition of DMQS at different concentrations is tabulated in Table 2.

$$\mathrm{IE_{IES}} = \frac{R_{ct} - R^0_{ct}}{R_{ct}} \times 100, \qquad (1)$$

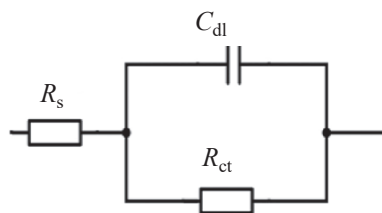The equivalent circuit contoured for the experimental data of EIS is depicted in Fig. 3, where C_{dl}, R_{ct}, and R_s are the capacitance of the double layer, the resistance of charge transfer and the resistance of solution respectively. The obtained values of the capacitance of the interface decreased with rise in concentration may be ascribed to the adsorption of the DMQS forming a protective adsorption layer on the carbon steel surface.
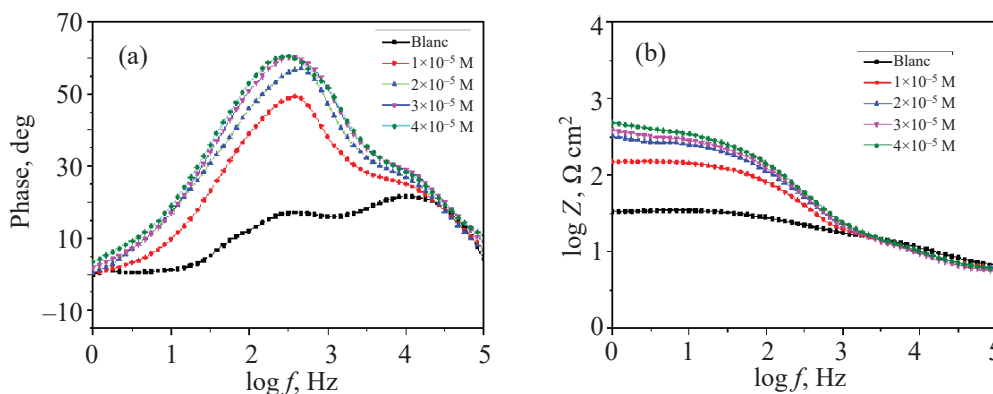
Fig. 4. (Color online) Bode plots (a) phase angle and (b) phase modulus for MS in 0.1 M HCl without the addition and with the addition of varied concentrations of DMQS at 303 K.

The resistance of charge transfer increases when there is a rise in inhibitor concentration, whereas it is observed to have decreased with the rise in temperature for a given concentration [15, 16]. The efficacy of inhibition improved with rise in concentration of the DMQS and declined with rise in temperature. The effect of inhibition relies on DMQS concentration and solution temperature. The results obtained from EIS studies prove DMQS to be an effectual inhibitor.

The bode plots without the addition and with the addition of varied concentrations of DMQS at 303 K is depicted in Fig. 4. From the bode plots it could be inferred that those electrochemical measurements fit aptly and presence of one relaxation process consents with the charge transfer process between the metal/electrolyte interface. The increase in phase angle with the concentration of DMQS implies development of a layer that is protective [17, 18].

Potentiodynamic polarization (PDP). The curves of potentiodynamic polarisation for MS consisting 0, 1 × 10^{-5}, 2 × 10^{-5}, 3 × 10^{-5}, and 4 × 10^{-5} M of the DMQS in 0.1 M HCl at 303, 313, and 323 K are shown in Fig. 5. Table 3 indicates the values of Potentiodynamic polarization (PDP) parameters at varied concentrations of DMQS with variation in temperature. The surface coverage (θ) and potentiodynamic polarization inhibition efficiency (IE$_{PDP}$, %) was determined employing the Eqs. 2 and 3, respectively [19], where i^0_{corr} is the corrosion current without the DMQS and i^i_{corr} is the corrosion current with the DMQS.

$$\theta = \frac{i^0_{corr} - i^i_{corr}}{i^0_{corr}}, \qquad (2)$$

$$\%IE_{PDP} = \frac{i^0_{corr} - i^i_{corr}}{i^0_{corr}} \times 100. \qquad (3)$$

There was a decline in the corrosion rate (CR) and corrosion current (i_{corr}) with rise in DMQS concentration implying the rise in the surface coverage leading to the formation of protective film between DMQS and MS surface by adsorption process. The surface inhibitor film shields the corrosive media from further attack thus delaying the evolution of hydrogen gas and dissolution

Table 2. Electrochemical impedance (EIS) parameters of MS in 0.1 M HCl at varied concentrations of DMQS with variation in temperature

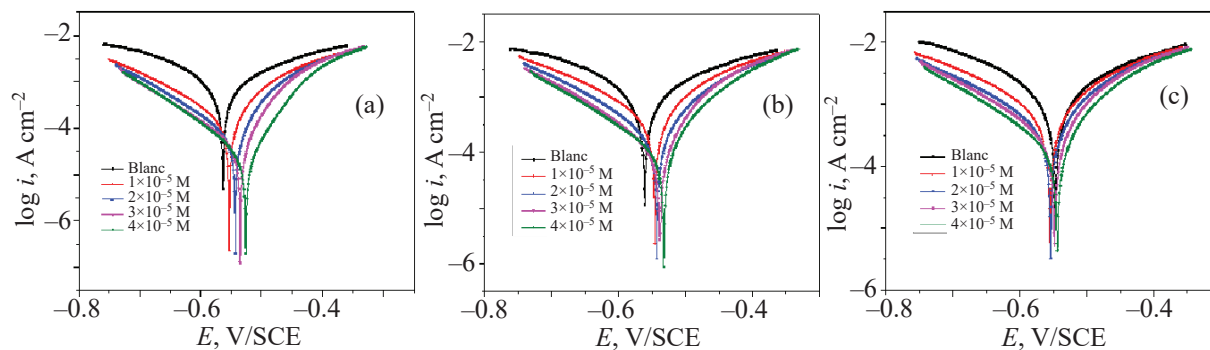| Temperature, K	Conc. of DMQS, M	R_{ct}, Ω cm²	C_{dl}, μF/ cm²	IE$_{EIS}$, %
303	Blank	29.40	241.53	–
	1 × 10^{-5}	142.30	199.54	79.34
	2 × 10^{-5}	303.10	19.89	90.30
	3 × 10^{-5}	368.70	13.76	92.03
	4 × 10^{-5}	468.60	13.07	93.73
313	Blank	21.63	218.58	–
	1 × 10^{-5}	57.29	193.84	62.24
	2 × 10^{-5}	102.50	75.21	78.90
	3 × 10^{-5}	151.60	33.26	85.73
	4 × 10^{-5}	183.30	19.42	88.20
323	Blank	19.64	128.39	–
	1 × 10^{-5}	43.36	108.16	54.70
	2 × 10^{-5}	60.66	46.37	67.62
	3 × 10^{-5}	80.97	30.56	75.74
	4 × 10^{-5}	107.80	14.66	81.78

Fig. 5. (Color online) Potentiodynamic polarization curves of MS in 0.1 M HCl without the addition and with the addition of different concentrations of DMQS at (a) 303, (b) 313, and (c) 323 K.

of the MS [20]. There are no exceptional changes in the deracination of the both Tafel slopes (cathodic slopes (β_c) and anodic slopes (β_a)) attributing to an adsorption process. The almost unchanged values of corrosion potential (E_{corr}) for varied concentrations implicate DMQS to be favouring the mixed type inhibition. The corrosion potential (E_{corr}) of DMQS solutions has decreased from that of the solution without the inhibitor and the displacement is less than 40 mV is tabulated in Table 3 which implies that the DMQS is a mixed type indicator. Mixed type inhibition implies suppression of the metal from undergoing dissolution and evolution of hydrogen gas, i.e., the anodic reaction and the cathodic reaction [21]. The data obtained in the EIS measurements are in good accord with the data obtained from the PDP measurements.

Temperature effect–adsorption isotherms. Temperature has a significant impact on the rate at which metal

would corrode and the EIS and PDP results are evidential in this regard [22–25]. It has been delineated that ascent in temperature advances the corrosion rate without and with the inhibitor in the case of MS but it is more expeditious in the blank solution [26]. The decline in the efficacy of DMQS with temperature rise ascribes to a chemical nature in the adsorption process. The study of temperature effect on the MS rate of corrosion in presence of DMQS is tendered through Arrhenius relationship [27]. The activation energy (E_a) for DMQS was determined by using Eq. 4, denoting A as Arrhenius constant, R as gas constant, T as the temperature and CR as the corrosion rate. Figure 6 depicts ln CR vs. reciprocal of absolute temperature plot that gives a line, i.e., linear in nature comprising a slope of E_a/R. The entropy of activation (ΔS^*) and enthalpy of activation (ΔH^*) were determined by using Eq. 5, denoting h as Plank's constant and N as Avogadro's number. Figure 7 depicts
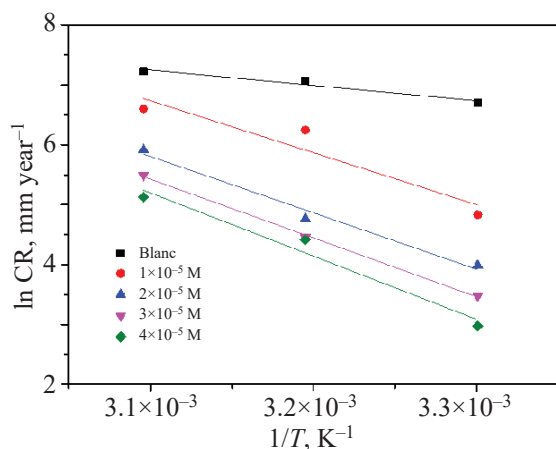

Fig. 6. (Color online) The plot of ln CR versus $1/T$ for MS corrosion in 0.1 M HCl without the addition and with the addition of DMQS.
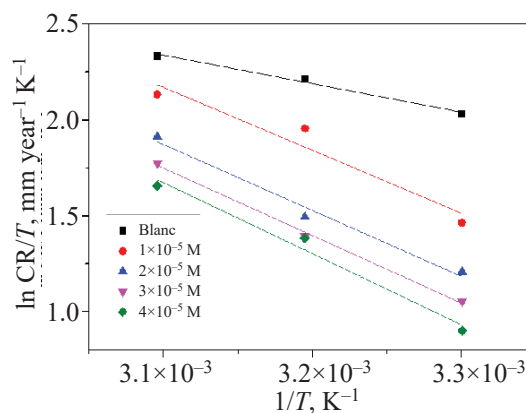

Fig. 7. (Color online) The plot of ln CR/T against $1/T$ for MS corrosion in 0.1 M HCl without the addition and with the addition of DMQS.

Table 3. Potentiodynamic polarization (PDP) data of MS in 0.1 M HCl at varied concentrations of DMQS with variation in temperature

Temperature, K	DMQS conc., M	β_c, mV	β_A, mV	i_{corr}, mA/cm^2	$-E_{corr}$, mV	CR, mil/year	IE$_{PDP}$, %
303	Blank	178.6	211.2	1.14	563	816.40	-
	1×10^{-5}	137.2	83.2	0.18	553	125.60	84.62
	2×10^{-5}	120.1	58.5	0.08	543	53.88	93.40
	3×10^{-5}	118.8	53.2	0.05	535	32.34	96.04
	4×10^{-5}	108.6	59.7	0.03	526	19.53	97.61
313	Blank	193.2	203.4	1.64	561	1177.00	–
	1×10^{-5}	213.1	154.9	0.72	546	517.20	56.16
	2×10^{-5}	136.4	88.9	0.25	543	117.86	84.86
	3×10^{-5}	123.9	67.2	0.12	539	85.97	92.72
	4×10^{-5}	127.0	67.6	0.11	533	82.78	92.99
323	Blank	192.6	202.6	1.92	552	1379.00	–
	1×10^{-5}	211.6	164.1	1.03	555	737.30	46.57
	2×10^{-5}	161.5	103.1	0.52	554	372.90	72.97
	3×10^{-5}	149.8	84.8	0.34	548	242.30	82.47
	4×10^{-5}	141.1	78.3	0.24	544	168.70	87.77

ln (CR/T) vs. reciprocal of absolute temperature plot that gave a line, i.e., linear in nature comprising $-\Delta H^*/R$ as slope and ln $R/Nh + \Delta S^*/R$ as an intercept.

$$\ln CR = A - \frac{E_a}{RT}, \qquad (4)$$

$$CR = \frac{RT}{Nh}\exp\frac{\Delta S^*}{R}\exp\frac{-\Delta H^*}{RT}. \qquad (5)$$

The activation parameter values obtained were tabulated in Table 4. The descried values of activation energies are above 70 kJ/mol, but below 100 kJ/mol and can be implied to mixed-type of adsorption which involves physisorption and chemisorption. This trend in activation parameters has been observed in sulfonamide studies carried out earlier by Murulana and Kabanda [28, 29]. The values E_a, ΔS^* and ΔH^* indicated an ascent with the rise in DMQS concentration. This could be ascribed to an increase in disorder amidst the relative adsorption process to an activated complex formation [30].

The adsorption study was carried out for DMQS and the regression coefficient values (r^2) obtained are near to 1 permit from the linear relationship of Langmuir pattern, so it was deduced that adsorption isotherm of Langmuir was the most befitting. The surface coverage

of the DMQS on the MS can be given by the Langmuir isotherm relationship in Eq. 6 [31–34], where, equilibrium constant is K_{ads} for the DMQS adsorption on MS and C$_{inh}$ is the molar concentration.

$$\frac{C_{inh}}{\theta} = \frac{1}{K_{ads}} + C_{inh}. \qquad (6)$$

Table 4. Activation Parameters of dissolution of MS in 0.1 M HCl without the addition and with the addition of varied concentrations of the DMQS

Concentration, M	E_a, kJ/mol	ΔH^*, kJ/mol	$-\Delta S^*$, J/mol/K
Blank	21.41	12.36	139.77
1×10^{-5}	72.44	27.32	94.82
2×10^{-5}	78.52	28.60	93.33
3×10^{-5}	81.88	29.27	92.28
4×10^{-5}	88.01	30.83	88.06

Table 5. Thermodynamic adsorption parameters of DMQS at varied temperatures on MS in 0.1 M HCl

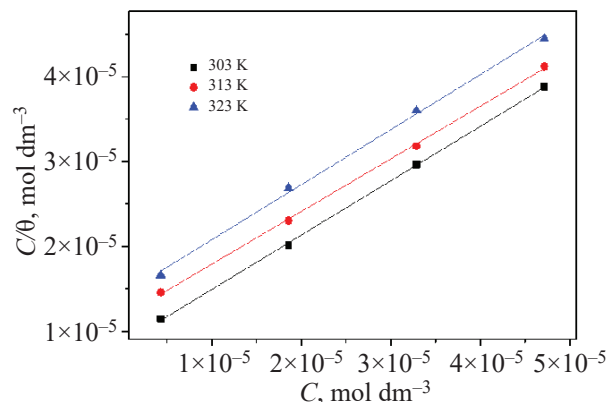| Temperature, K	r^2	Slope	K_{ads}, M^{-1}	ΔG^0_{ads}, kJ mol^{-1}
303	0.999	1.007	4.275	–42.78
313	0.999	0.975	1.654	–41.72
323	0.997	1.019	1.161	–42.10

Fig. 8. (Color online) Langmuir adsorption isotherms for the corrosion of MS in 0.1 M HCl at varied temperatures.

Fig. 9. Interaction of DMQS on MS in 0.1 M HCl by physisorption and chemisorption.

The depiction of thermodynamic parameters for the adsorption of DMQS are tabulated in Table 5. The Langmuir adsorption isotherm is depicted in Fig. 8. Using Eq. 7 the standard free energy is calculated from the adsorption equilibrium constant values, where ΔG^0_{ads} is the standard free energy and in the solution the molar concentration of water is represented by the value of 55.5 [35]. There are studies associated to the values of ΔG^0_{ads} ranging from –40 kJ mol^{-1} and more correlated to chemisorption, i.e., charge sharing or transfer of electrons, whereas values of ΔG^0_{ads} ranging from –20 kJ mol^{-1} and below as physisorption, i.e., electrostatic interaction [36–38]. The process of chemisorption could be corresponded for DMQS as the ΔG^0_{ads} values attained are more than –40 kJ mol^{-1}.
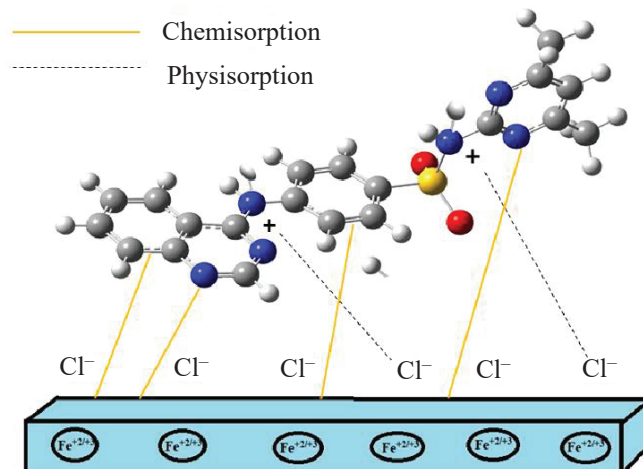
$$\Delta G^0_{ads} = -RT \ln(55.5 K_{ads}). \qquad (7)$$

The adsorption of DMQS on MS is depicted in Fig. 9 is a possible outcome of interaction between the MS and the hetero atoms through π electron. The adsorption could also be due to electrostatic interaction between MS and the protonated molecule of DMQS. The hydrochloric acid media leads to Cl$^-$ ions being adsorbed on electrode surface to form a negatively charged mild steel surface that attracts the positively charged DMQS molecule thus leading to electrostatic interaction [39, 40].

SEM and EDS analysis. The images of SEM were taken and the EDS analysis of the MS surface with and without the DMQS was done to validate the development of a protective layer. Earlier studies have revealed that a stable film formation by the inhibitor protects the surface of the metal and supports the results obtained from electrochemical measurements [41–43]. The surface was soaked 0.1M HCl for 24 h at 303K and
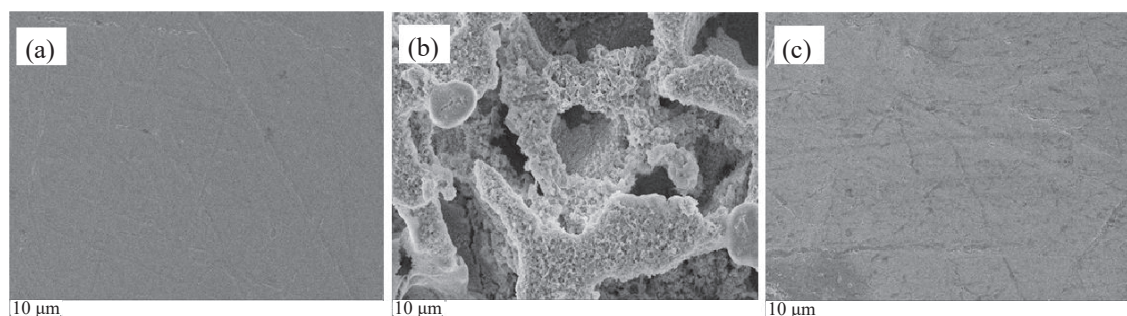

Fig. 10. SEM images of (a) smoothened surface of MS, (b) surface of MS in 0.1 M HCl solution, and (c) surface of MS in 0.1 M HCl containing 4×10^{-5} M DMQS.

Fig. 11. EDS analysis of (a) Smoothened surface of MS (b) Surface of MS in 0.1 M HCl solution and (c) Surface of MS in 0.1 M HCl containing 4×10^{-5} M DMQS.
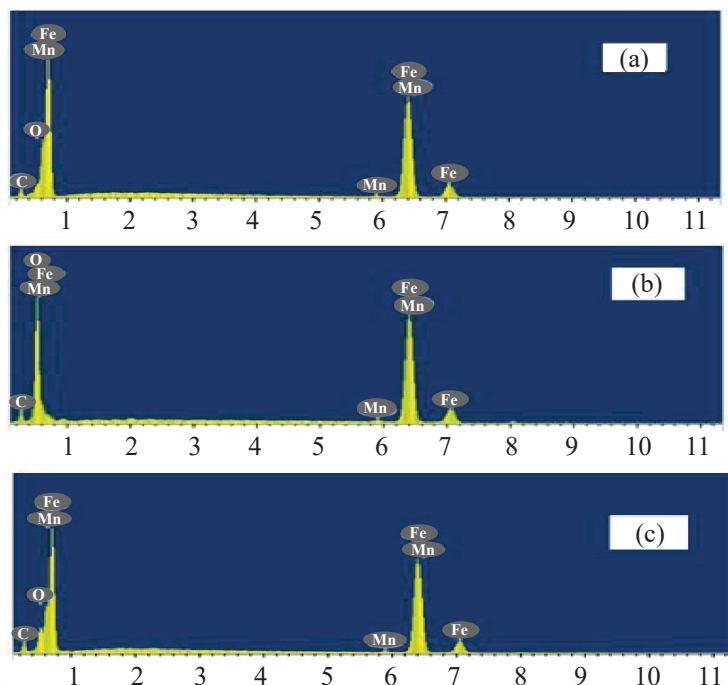
Fig. 10 shows the SEM images of the smoothened surface of MS, surface of MS soaked in 0.1 M HCl without the DMQS and surface of MS soaked in 0.1 M HCl containing 4×10^{-5} M DMQS. The images of SEM reveal that DMQS provides significant protection to mild steel.

The EDS analysis results revealed that the percentage of Iron decreased from 91.68% in the polished MS surface to 41.27% in the metal surface soaked in 0.1 M HCl without DMQS for a soaking time of 24 h. The percentage of Iron was 77.99% in the presence of DMQS on the MS surface for a 24 h soaking time. The EDS analysis images are shown in Fig. 11 which implicates that DMQS suppresses the corrosion rate of the MS surface. The MS surface without DMQS shows severe corrosion. The percentage of elemental composition of smoothened MS, surface of MS in 0.1 M HCl solution and surface of MS in 0.1 M HCl containing 4×10^{-5} M DMQS is displayed in Table 6.

Computational methods. The DFT method has been used extensively by researchers to understand the inhibition mechanism and illustrate the structural nature of the inhibitor [44–47]. The geometrical optimized structure of the DMQS is shown in Fig. 12. The prediction of adsorption centers on the DMQS is done from the values obtained through the frontier molecular orbitals
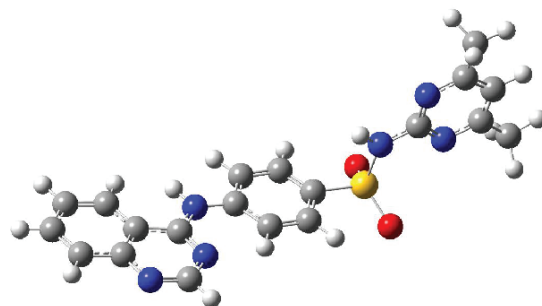

Fig. 12. Optimised structure of DMQS.

i.e., HOMO and LUMO. Structure of DMQS showing dissemination of HOMO energy and LUMO energy is displayed in Fig. 13. Eqs. 8 and 9 show that the ionization potential (I) and electron affinity (A) are similar to

Table 6. Composition of mild steel (weight %) of (a) smoothened surface of MS (b) surface of MS in 0.1 M HCl solution and (c) surface of MS in 0.1 M HCl containing 4×10^{-5} M DMQS

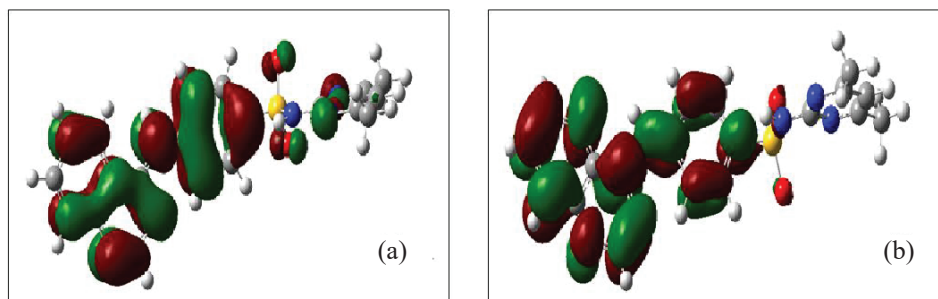| Element	Weight %		
	(a)	(b)	(c)
Fe	91.68	41.27	77.99
O	5.18	38.85	14.29
Mn	0.55	0.45	0.58
C	2.59	19.43	7.14

Fig. 13. Structure of DMQS showing distributions of (a) HOMO energy and (b) LUMO energy.
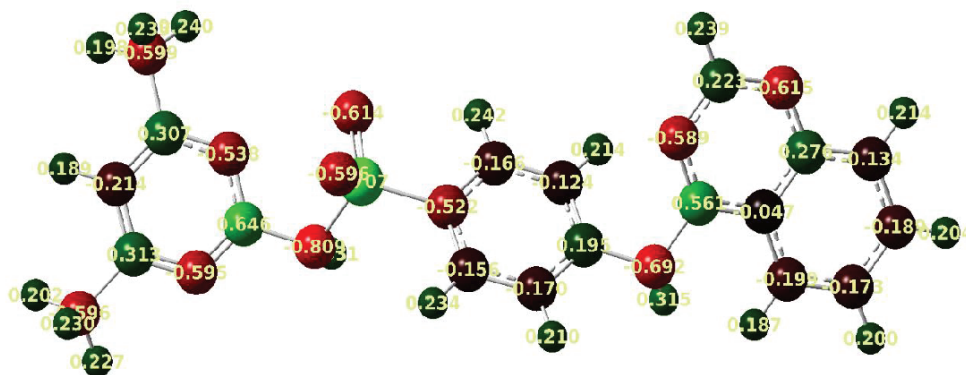

Fig. 14. Structure of DMQS with Mulliken charges on the optimised structure of DMQS.

the HOMO and the LUMO orbital energies of the inhibitor molecule as stated in Koopman's theorem [48, 49].

$$I = -E_{HOMO}, \quad (8)$$

$$A = -E_{LUMO}, \quad (9)$$

The parameters relative to quantum chemical calculations namely, energy gap (ΔE), electronegativity (χ),

Table 7. DFT at B3LYP//3-21G employed for DMQS quantum chemical calculations

Parameters	Value
E_{HOMO}, eV	−6.25672
E_{LUMO}, eV	−1.90262
ΔE, eV	4.35410
Ionization potential I, eV	6.25672
Electron affinity A, eV	1.90262
Dipole moment μ, Debye	6.53870
Electronegativity χ, eV	4.07970
Global hardness η, eV	2.17705
Softness S, eV^{-1}	0.45934
ΔN	0.67070
ω, eV	4.35410

global hardness (η), fraction of electrons transferred (ΔN), Softness (S) and electrophilicity (ω) were determined using Eqs. 10–15 [50, 51] and are shown in Table 7.

$$\Delta E = E_{LUMO} - E_{HOMO}, \quad (10)$$

$$\chi = \frac{-(E_{LUMO} + E_{HOMO})}{2}, \quad (11)$$

$$\eta = \frac{E_{LUMO} - E_{HOMO}}{2}, \quad (12)$$

$$\Delta N = \frac{\chi_{Fe} - \chi_{inh}}{[2(\eta_{Fe} + \eta_{inh})]}, \quad (13)$$

$$S = \frac{1}{\eta}, \quad (14)$$

$$\omega = \frac{\mu^2}{2\eta}. \quad (15)$$

The E_{HOMO} of the inhibitor is relative with the capacity to donate electrons and a higher negative value indicates greater tendency to donate electron by getting adsorbed on the surface. The value of large energy gap in the molecule are considered to be stable and the one with small energy gap are considered to be reactive with good inhibition efficiency [52, 53]. The E_{HOMO} value of

Table 8. Atoms of the DMQS molecule showing mulliken charge (B3LYP/ 3-21G (d, p) results in vacuo)

Individual atom	Mulliken charge	Individual atom	Mulliken charge	Individual atom	Mulliken charge
C 1	–0.178425	C 17	–0.169618	C 33	0.298557
C 2	–0.165071	H 18	0.177448	**N 34**	**–0.584420**
C 3	**–0.509441**	C 19	–0.147796	C 35	–0.225221
C 4	–0.154956	C 20	–0.187754	H 36	0.183227
C 5	–0.200621	H 21	0.200570	**C 37**	**–0.589278**
C 6	0.344846	H 22	0.216186	H 38	0.224242
H 7	0.256112	H 23	0.203676	H 39	0.194802
H 8	0.239396	**N 24**	**–0.620306**	H 40	0.224993
H 9	0.240320	**N 25**	**–0.580792**	**C 41**	**–0.590040**
H 10	0.188291	C 26	0.227486	H 42	0.234012
N 11	**–0.897066**	H 27	0.226383	H 43	0.234429
H 12	0.336938	**N 28**	**–0.908938**	H 44	0.190540
C 13	0.699122	H 29	0.356791	**O 45**	**–0.543739**
C 14	–0.006492	C 30	0.803122	**O 46**	**–0.549155**
C 15	–0.216569	**N 31**	**–0.596711**	**S 47**	**1.599282**
C 16	0.237800	C 32	0.283838		

DMQS infers that it has large potential to donate electrons towards the metal surface. The energy gap value infers good inhibition efficiency. The prediction of inhibitory efficacy of inhibitor is done through finding the dipole moment (μ), i.e., inhibitor showing sturdy dipole-dipole interactions with the metal surface [10]. DMQS has a dipole moment value of 6.5424 Debye inferring it to be an effectual inhibitor. The global softness value of DMQS is 0.459 eV^{-1} inferring its behaviour as a soft base inhibitor providing good adsorption with the metal atoms. The parameter for global chemical reactivity is known to be electrophilicity index (ω) [54]; A high value indicates that the inhibitor is a good electrophile and low value indicates it to be a good nucleophile.

The Structure of DMQS with Mulliken charges on the optimised structure is shown in Fig. 14. Obot et al. and Elmsellem et al. have reported that the atoms of the absorbed center having atomic charge with higher negative value will have extra feasibility in donating its electrons to the metal's unoccupied orbital [55, 56]. Table 8 exhibits the mulliken charges on the atom of the DMQS molecule and it is observed that the nitrogen atoms (N11, N24, N25, N28, N31 and N34) have high negative values inferring them to be the highest active sites for the adsorption of iron. The nitrogen atoms N11 and N28 have the highest negative value, i.e., –0.8970 and –0.9089 respectively, implying they have three bonds

already and cannot form another bond. The carbon atoms (C3, C37 and C41) and oxygen atoms connected to sulphur atom (O45 and O46) show high negative value indicating them as highly reactive sites to allow the adsorption on mild steel.

CONCLUSIONS

N-(4,6-Dimethylpyrimidin-2-yl)-4-[(quinazoline-4-yl)amino]benzene-1-sulfonamide has been investigated and has proved its effectuality in corrosion inhibition for MS in aq. HCl by experimental and computational studies. Electrochemical impedance spectroscopy established that the inhibitory efficacy had increased appreciably with increased concentration of the DMQS and declined relatively with increment in temperature. The measurements of potentiodynamic polarization rendered DMQS to be a mixed type inhibitor. Langmuir adsorption isotherm was obeyed by DMQS indicating the relative adsorption process to an activated complex formation. Retention of 77.99% of iron content in MS indicated the development of a protective layer in the presence of DMQS on the surface of MS that was confirmed through the EDS and SEM analysis. The Mulliken charges on the optimised molecule of DMQS show high negative values on the hetero atoms implying they are highly reactive sites to allow the adsorption on

mild steel. The molecular quantum calculation results validated the efficacy of the inhibitor which equates to the experimental results. Organic inhibitors like DMQS with high inhibitory efficiency offer the scope to manifest its applicability in protection of constructional materials with the added advantage of being environmentally affable.

ACKNOWLEDGMENTS

REFERENCES

1. Fouda, A.S. and Hassan, H.M., *Int. J. Electrochem. Sci.*, 2013, vol. 8, pp. 5866–5885.
https://doi.org/10.20964/2017.06.66

2. Obi-Egbedi, N.O., Obot, I.B., and Eseola, A.O., *Arab. J. Chem.*, 2014, vol. 7, no. 2, pp. 197–207.
https://doi.org/10.1016/j.arabjc.2010.10.025

3. Ebenso, E.E., Arslan, T., Kandemirli, F., et al., *Int. J. Quantum. Chem.*, 2010, vol. 110, no. 14, pp. 2614-2636.
https://doi.org/10.1002/qua.22430

4. Stohs, S.J., and Miller, M.J.S., *Food. Chem. Toxicol.*, 2014, vol. 63, pp. 240–243.
https://doi.org/10.1016/j.fct.2013.11.008.

5. Gen, Y., Ozkanca, R., and Bekdemir, Y., *Ann. Clin. Microbiol.*, *Antimicrob.*, 2008, vol. 7, pp. 1–6.
https://doi.org/10.1186/1476-0711-7-17

6. Pisanenko, D.A., Klimko, Y.E., and Likhnitskii, K.V., *Russ. J. Appl. Chem.*, 2011, vol. 84, no. 8, pp. 1445–1447.
https://doi.org/10.1134/S1070427211080283

7. Kumar, A.S., Kudva, J., Bharath, B.R., et al., *Chemistry Select.*, 2018, vol. 3, no. 48, pp. 13586–13595.
https://doi.org/10.1002/slct.201802402

8. Kumar, A.S., Kudva, J., Lahtinen, M., et al., *J. Mol. Struct.*, 2019, vol. 1190, pp. 29–36.
https://doi.org/10.1016/j.molstruc.2019.04.050

9. Kumar, A.S., Kudva, J., Bharath, B.R., et al., *New. J. Chem.*, vol. 2019, vol. 43, no. 3, pp. 1597–1610.
https://doi.org/10.1039/c8nj03671c

10. Udhayakala, P., *J. Chem. Pharm. Res.*, 2014, vol. 6, no. 7, pp. 117–127.
https://www.researchgate.net/publication/268444605.

11. Yadav. M., Kumar, S., Sinha, R.R., et al., *J. Mol. Liq.*, 2015, vol. 211, pp. 135–145.
https://doi.org/10.1016/j.molliq.2015.06.063

12. Raviprabha, K., and Bhat, R.S., *J. Fail. Anal. Prev.*, 2019, vol. 19, pp. 1464–1474.
https://doi.org/10.1007/s11668-019-00744-5

13. Wang, B., Du, M., Zhang, J., and Gao, C.J., *Corros. Sci.,* 2011, vol. 53, no. 1, pp. 353–361.
https://doi.org/10.1016/j.corsci.2010.09.042

14. Laamari, R., Benzakour, J., Berrekhis, F., Abouelfida, A., Derja, A., and Villemin, D., *Arab. J. Chem.*, 2011, vol. 4, no. 3, pp. 271–277.
https://doi.org/10.1016/j.arabjc.2010.06.046

15. Tourabi, M., Nohair, K., Traisnel, M., et al., *Corros Sci.*, 2013, vol. 75, pp. 123–133.
https://doi.org/10.1016/j.corsci.2013.05.023

16. Kord, L., and Nasr-Esfahani, M., *Surf. Eng. Appl. Electrochem.*, 2015, vol. 51, no. 5, pp. 491–500.
https://doi.org/10.3103/S1068375515050087

17. Shenoy, K.V., Venugopal, P.P., Kumari, P.D.R., and Chakraborty, D., *J. Mol. Struct.*, 2021, vol. 1232, no. 130074.
https://doi.org/10.1016/j.molstruc.2021.130074

18. Espinoza-Vazquez, A., Rodriguez-Gomez, F.J., Martínez-Cruz, I.K., et al., *R. Soc. Open Sci.*, 2019, vol. 6, no. 181738.

19. Preethi, K.P., Shetty, P., and Rao, S.A., *Arab. J. Chem.*, 2017, vol. 10, no. 5, pp. 653–663.
https://doi.org/10.1016/j.arabjc.2014.09.005

20. John, S., Jeevana, R., Aravindakshan, K.K., and Joseph, A., *Egypt J Pet.*, 2017, vol. 26, pp. 2405–2412.
https://doi.org/10.1016/j.ejpe.2016.05.012

21. Prasanna, B.M., Praveen, B.M., Hebbar, N., et al., *J. Assoc. Arab. Univ. Basic. Appl. Sci.*, 2017, vol. 22, pp. 62–69.
https://doi.org/10.1016/j.jaubas.2015.11.001

22. Esmaily, M., Shahabi-Navid, M., Svensson, J.E., et al., *Corros Sci.*, 2015, vol. 90, pp. 420–433.
https://doi.org/10.1016/j.corsci.2014.10.040

23. Chakravarthy, M.P., Mohana, K.N., and Pradeep, K.C.B., *Int. J. Ind. Chem.*, 2014, vol. 5, no. 2, pp. 1–21.
https://doi.org/10.1007/s40090-014-0019-3

24. Singh, A., Ansari, K.R., Quraishi, M.A., et al., *J. Alloys. Compd.,* 2018, vol. 762, pp. 347–362.
https://doi.org/10.1016/j.jallcom.2018.05.236

25. Mishra, A., Verma, C., Lgaz, H., et al., *J. Mol. Liq.*, 2018, vol. 251, no. 317–332.
https://doi.org/10.1016/j.molliq.2017.12.011

26. Bouklah, M., Benchat, N., Aouniti, A., et al., *Prog. Org. Coatings.*, 2004, vol. 51, no. 2, pp. 118–124.
https://doi.org/10.1016/j.porgcoat.2004.06.005

27. Abeng, F.E., Idim, V.D., Obono, E.O., and Magu, T.O., *World. News. Nat. Sci.*, 2017, vol. 77, no. 2, pp. 298–313.
https://www.researchgate.net/publication/317952063.

28. Murulana, L.C., Kabanda, M.M., and Ebenso, E.E., *RSC*

Adv., 2015, vol. 5, no. 36, pp. 28743–28761.
https://doi.org/10.1039/c4ra11414k

29. Murulana, L.C., Kabanda, M.M., and Ebenso, E.E., *J. Mol. Liq.*, 2016, vol. 215, pp. 763–79.
https://doi.org/10.1016/j.molliq.2015.12.095

30. Singh, A.K., and Quraishi, M.A., *Corros. Sci.*, 2010, vol. 52, no. 4, pp. 1373–1385.
https://doi.org/10.1016/j.corsci.2010.01.007

31. Singh, A.K., and Quraishi, M.A., *Corros. Sci.*, 2011, vol. 53, no. 4, pp. 1288–1297.
https://doi.org/10.1016/j.corsci.2011.01.002

32. Singh, A.K., and Quraishi, M.A., *Corros. Sci.*, 2010, vol. 52, no. 1, pp. 152–160.
https://doi.org/10.1016/j.corsci.2009.08.050

33. Shihab, M.S., and Mahmood, A.F., *Russ. J. Appl. Chem.*, 2016, vol. 89, no. 3, pp. 505–516.
https://doi.org/10.1134/S1070427216003023X

34. He, Y., Zhou, Y., Yang, R., et al., *Russ. J. Appl. Chem.*, 2015, vol. 88, no. 7, pp. 1192–1200.
https://doi.org/10.1134/S1070427215070149

35. Amin, M.A., *J. Appl. Electrochem.*, 2006, vol. 36, no. 2, pp. 215–226.
https://doi.org/10.1007/s10800-005-9055-1

36. Piccin, J.S., Dotto, G.L., and Pinto, L.A.A., *Brazilian. J. Chem. Eng.*, 2011, vol. 28, no. 2, pp. 295–304.
https://doi.org/10.1590/S0104-66322011000200014

37. Abdallah, M., Salem, M.M., Jahdaly, B.A.A., et al., *Int. J. Electrochem. Sci.*, 2017, vol. 12, pp. 4543–4562.
https://doi.org/10.20964/2017.05.35

38. Ituen, E., Akaranta, O., and James, A., *Chem. Sci. Int. J.*, 2017, vol. 18, no. 1, pp. 1–34.
https://doi.org/10.9734/csji/2017/28976

39. Goyal, M., Kumar, S., Bahadur, I., et al., *J. Mol. Liq.*, 2018, vol. 256, pp. 565–573.
https://doi.org/10.1016/j.molliq.2018.02.045

40. Al, M.K., Elmsellem, H., Sebbar, N.K., et al., *J. Mater. Environ. Sci.,* 2016, vol. 7, no. 9, pp. 3286–3299.
https://www.researchgate.net/publication/307980973

41. Bentiss, F., Traisnel, M., Gengembre, L., and Lagrenee, M., *Appl. Surf. Sci.*, 1999, vol. 152, no. 3, pp. 237–249.
https://doi.org/10.1016/S0169-4332(99)00322-0

42. Zhao, P., Liang, Q., and Li, Y., *Appl. Surf. Sci.*, 2005, vol. 252, no. 5, pp. 1596–1607.
https://doi.org/10.1016/j.apsusc.2005.02.121

43. Amin, M.A., Abd, E.S.S., El-Sherbin, E.E.F., and Bayoumi, R.S., *Electrochim. Acta.*, 2007, vol. 52, no. 11, pp. 3588–3600.
https://doi.org/10.1016/j.electacta.2006.10.019

44. Zarrouk, A., Ouali, I.E., Bouachrine, M., et al., *Res. Chem. Intermed.*, 2013, vol. 39, pp. 1125–1133.
https://doi.org/10.1007/s11164-012-0671-1

45. Fergachi, O., Benhiba, F., Rbaa, M., et al., *Mater Res.*, 2018, vol. 21, no. 6, pp. 1–11.
https://doi.org/10.1590/1980-5373-MR-2017-1038

46. Kabanda, M.M., Murulana, L.C., and Ebenso, E.E., *Int. J. Electrochem. Sci.,* 2012, vol. 7, no. 8, pp. 7179–7205.
https://www.researchgate.net/publication/231338432.

47. Farhadian, A., Rahimi, A., Safaei, N., et al., *Corros. Sci.*, 2020, vol. 175, no. 108871.
https://doi.org/10.1016/j.corsci.2020.108871

48. Martinez, S., *Mater. Chem. Phys.*, 2002, vol. 77, pp. 97–102.
https://doi.org/10.1016/S0254-0584(01)00569-7

49. Kumar, C.B.P., Prashanth, M.K., Mohana, K.N., et al., *Surf. Interfaces.*, 2020, vol. 18, no. 100446.
https://doi.org/10.1016/j.surfin.2020.100446

50. Issa, R.M., Awad, M.K., and Atlam, F.M., *Mater. Corros.*, 2010, vol. 8, pp. 709–714.
https://doi.org/10.1002/maco.200905361

51. Bashir, S., Lgaz, H., Chung, I., and Kumar, A., *Chem. Pap.,* 2019, vol. 73, no. 9, pp. 2255–2264.
https://doi.org/10.1007/s11696-019-00775-0

52. Reena, K.P.D., and Kumari, D., *J. Fail. Anal. Prev.*, 2018, vol. 18, no. 4, pp. 856–867.
https://doi.org/10.1007/s11668-018-0473-x

53. Fu, L., Yi, F., Zeng, B., et al., *Russ. J. Appl. Chem.,* 2018, vol. 91, no. 3, pp. 499–509.
https://doi.org/10.1134/S1070427218030242

54. Efil, K., and Bekdemir, Y., *Am. J. Phys. Chem.*, 2014, vol. 3, no. 2, pp. 19–25.
https://doi.org/10.11648/j.ajpc.20140302.13

55. Obot, I.B., Obi-Egbedi, N.O., and Eseola, A.O., *Ind. Eng. Chem. Res.*, 2011, vol. 50, pp. 2098–2110.
https://www.researchgate.net/publication/331873161

56. Elmsellem, H., Youssouf, M.H., Aouniti, A., et al., *Russ. J. Appl. Chem.,* 2014, vol. 87, no. 6, pp. 744–753.
https://doi.org/10.1134/S1070427214060147